ELSEVIER

Earth and Planetary Science Letters 161 (1998) 85–100

EPSL

Subsidence and growth of Pacific Cretaceous plateaus

Garrett Ito [a,*], Peter D. Clift [b]

[a] School of Ocean and Earth Science and Technology, POST 713, University of Hawaii at Manoa, Honolulu, HI 96822, USA
[b] Department of Geology and Geophysics, Woods Hole Oceanographic Institution, Woods Hole, MA 02543, USA

Received 10 November 1997; revised version received 11 May 1998; accepted 4 June 1998

Abstract

The Ontong Java, Manihiki, and Shatsky oceanic plateaus are among the Earth's largest igneous provinces and are commonly believed to have erupted rapidly during the surfacing of giant heads of initiating mantle plumes. We investigate this hypothesis by using sediment descriptions of Deep Sea Drilling Project (DSDP) and Ocean Drilling Program (ODP) drill cores to constrain plateau subsidence histories which reflect mantle thermal and crustal accretionary processes. We find that total plateau subsidence is comparable to that expected of normal seafloor but less than predictions of thermal models of hotspot-affected lithosphere. If crustal emplacement was rapid, then uncertainties in paleo-water depths allow for the anomalous subsidence predicted for plumes with only moderate temperature anomalies and volumes, comparable to the sources of modern-day hotspots such as Hawaii and Iceland. Rapid emplacement over a plume head of high temperature and volume, however, is difficult to reconcile with the subsidence reconstructions. An alternative possibility that reconciles low subsidence over a high-temperature, high-volume plume source is a scenario in which plateau subsidence is the superposition of (1) subsidence due to the cooling of the plume source, and (2) uplift due to prolonged crustal growth in the form of magmatic underplating. This prolonged crustal growth and uplift scenario may explain the low and thus submarine relief during plume initiation, the late stage eruptions found on Ontong Java (90 Ma) and Manihiki (~70 Ma), a large portion of the high-seismic-velocity lower crust, and the widespread normal faults observed throughout and along the margins of the three plateaus. Such late stage underplating may have occurred continuously or in discrete stages over ~30 m.y. and implies lower magmatic fluxes than previously estimated.

Keywords: subsidence; underplating; hot spots; flood basalts; West Pacific Ocean Islands; East Pacific Ocean Islands; mantle plumes

1. Introduction

Ontong Java and Manihiki Plateaus, together with the Shatsky Rise, are among the largest of the world's igneous provinces. Due to their great size and possible high eruption rates [1,2], the formation of these plateaus may represent a mode of mass and heat transfer from the mantle to the Earth's surface in the Cretaceous that was very different than those active at present-day. A hotspot-type origin, explained as the surfacing of a hot mantle convection plume at the base of the lithosphere, has become widely accepted. One type of hotspot model that has gained support attributes the high igneous volume and eruption rates to the surfacing and melting of giant heads of initiating mantle plumes (e.g. [3,4]). This model suggests an extreme mantle source with

* Corresponding author. Tel: +1 808 956 4777; Fax: +1 808 956 5512; E-mail: gito@soest.hawaii.edu

0012-821X/98/$19.00
PII S0012-821X(98)00139-3

temperature anomalies as high as ~350ºC [4,5] and an initial radius of ~400 km [1,5] which eventually spreads beneath the lithosphere over lateral distances of ~2000 km [4]. In contrast, less extreme hotspot models advance a more continuous growth history involving a long-lasting mantle plume rising beneath an already volcanically active oceanic spreading center, as in the case of Iceland [6,7].

The association of these features with hotspots predicts anomalous uplift of the regional seafloor in the form of a "hotspot swell" [8,9]. The hotspot swell then subsides rapidly as the anomalously high mantle temperatures diminish, and the swell eventually disappears [9–11]. The other main source of topographic variation is igneous emplacement itself, which after it is complete, causes permanent topography that we observe today as the oceanic plateaus. Thus, plateau subsidence histories — as revealed by the nature of sediments that have accumulated on top of plateaus — can provide constraints on the mantle thermal as well as crustal accretionary evolution.

In this study, we compile sediment descriptions from DSDP/ODP Sites 288, 289, 803, and 807 on Ontong Java, Site 317 on Manihiki, and Site 305 on the Shatsky Rise, which penetrated to or near basement. We then examine the depths of sedimentation since the time of basement emplacement, and estimate the sediment-unloaded isostatic depth of igneous basement in order to isolate the vertical trajectories of the plateaus as driven only by mantle and accretionary processes. Next, we compare estimates of total subsidence with predictions of thermal models of plume-influence lithosphere, and finally, examine the implications as to the nature of the mantle source, the style of plateau accretion, as well as possible causes of post-emplacement tectonism.

2. Tectonic setting

2.1. Ontong Java Plateau

The Ontong Java Plateau may be the largest flood basalt province in the world [1] (Fig. 1b). Its broad and relatively flat surface stands ~3 km above the surrounding seafloor as supported isostatically [12] by a thick (>25 km) igneous crust [13–15]. Basalts sampled at DSDP Site 289 and ODP Site 807 [16] (Fig. 1b), as well as on the Solomon Islands of Malaitia and Santa Isabel [17], yield $^{40}Ar/^{39}Ar$ dates of ~122 Ma, indicating that an Early Cretaceous magmatic event spanned an area comparable to that of the entire modern plateau. Other samples on Santa Isabel [17] and at ODP Site 803 [16] yield an age of ~90 Ma, indicating a later constructional event that spanned an area equally as broad.

Ontong Java may have formed at or near a mid-ocean ridge as suggested by findings of geochemical signatures that are characteristic of mid-ocean ridge basalts (MORB) [7], as well as major and trace element compositions suggestive of high extents of partial melting [16,17]. Indeed, the Nauru Basin magnetic lineations across from the drill sites range from M10 (131 Ma [18]) near Site 288 to M26 (~155 Ma [18]) near Site 807, thus suggesting these sites may have erupted on relatively young seafloor only 9–33 m.y. old. These estimates for pre-existing seafloor ages, however, assume no offset in seafloor ages between the Nauru Basin where in fact the presence of ridge segment offsets has been proposed by other workers [15,19]. Finally, block faulting as imaged seismically [14,20] and inferred from satellite gravity images [21] (Fig. 1b), may indicate rifting and transform tectonics associated with a mid-ocean ridge. We will discuss a possible alternative mechanism for faulting below.

2.2. Manihiki Plateau

The Manihiki Plateau spans an area approximately a third as broad as Ontong Java (Fig. 1c). Its elevation of 2–3 km above the surrounding abyssal seafloor is supported by a crust ~21 km in thickness [14]. Faulting within and along the margins of Manihiki indicate crustal extension, possibly related to rifting at either the Pacific–Antarctic spreading center or the Pacific–Antarctic–Farallon triple junction during Manihiki's formation [22]. In satellite gravity images [21], these tectonic features are evident as linear highs and lows within and surrounding the plateau (Fig. 1c). Tarduno et al. [2] argued that Manihiki formed at approximately the same time as Ontong Java (early Aptian), and was also as a result of rapid flood volcanism. The only drill core that reached basement (DSDP Site 317) yields a

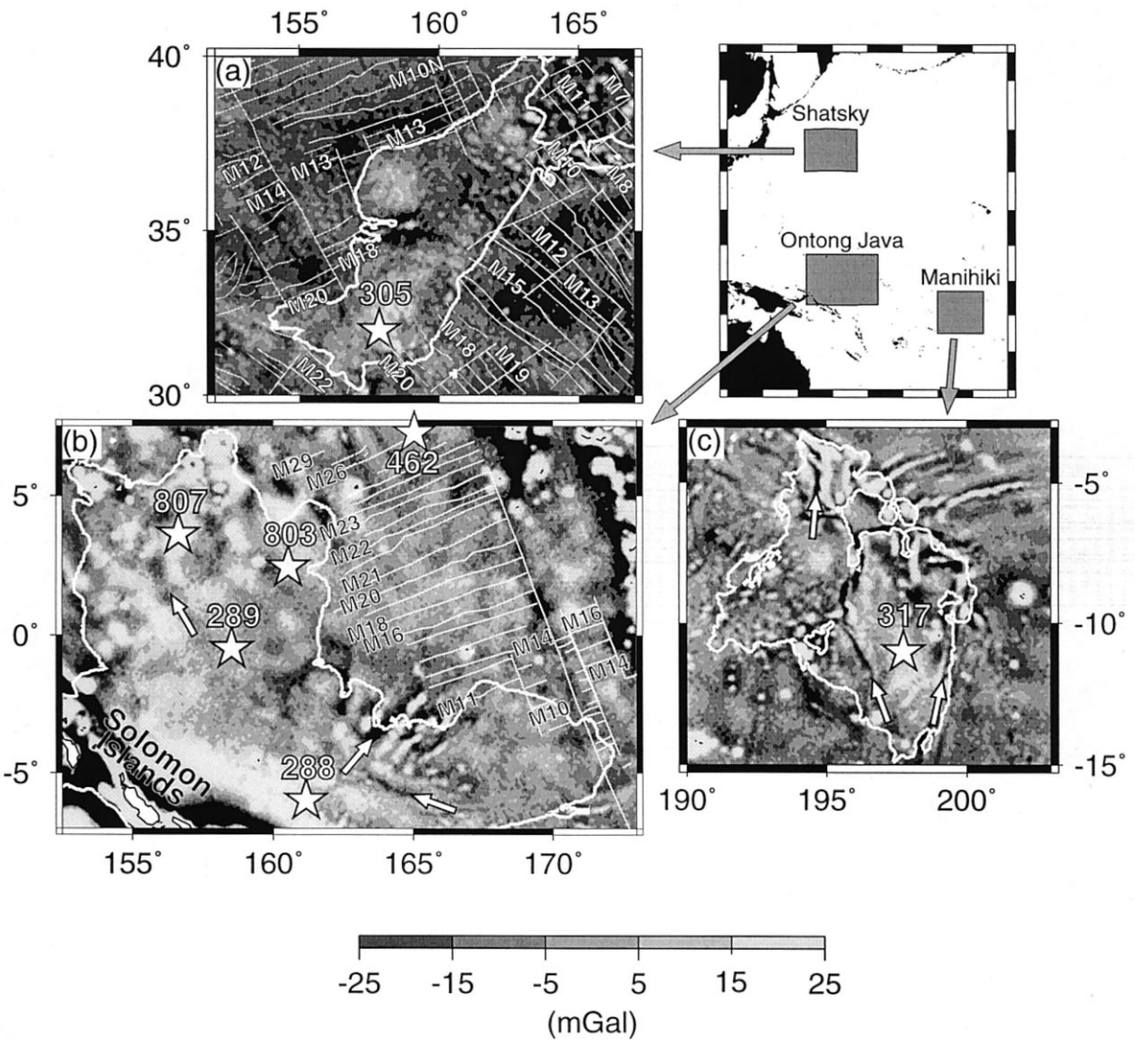

Fig. 1. Satellite-derived gravity maps [21] of (a) Shatsky Rise, (b) Ontong Java Plateau, and (c) Manihiki Plateau in the western Pacific. White contours outline ETOPO5 depths of (a) 5100 m, (b) 4000 m, and (c) 4500 m. The locations of the ODP and DSDP drill sites are marked with stars, and magnetic lineations of the surrounding seafloor are marked [26,27]. Arrows point to examples of linear gravity features which may reflect crustal normal faults. The Solomon Islands on Ontong Java are in the southwest corner of (a).

date of 106 ± 3.5 Ma [23]; however, the K–Ar dating method used is less reliable than methods of $^{40}Ar/^{39}Ar$ dating as confirmed by overlying sediments that date from the Aptian *L. cabri* planktonic foraminifer zone [24], or ~118 Ma. Given the available age constraints of the plateau and the fact that the surrounding seafloor formed during the Cretaceous magnetic quiet zone (83–123 Ma), Manihiki most likely erupted on very young lithosphere (0–10 m.y.), consistent with a near-ridge origin.

2.3. Shatsky Rise

The Shatsky Rise, in the northwestern Pacific, is comparable to Manihiki in both elevation, area [25], and crustal thickness [14]. Magnetic anomalies

surrounding the Shatsky Rise [26,27] provide compelling evidence that Shatsky originated on or near a Mesozoic triple junction [28] (Fig. 1a). Sager and Han's [28] analysis of plateau magnetism suggested that the southern portion of the plateau erupted during a single Early Cretaceous polarity interval that lasted no more than ~1.2 m.y. The implied eruption rate of 1.7 km^3/y is consistent with a flood basalt origin. No radiometric age data is available from either DSDP Site 305 or 306, however, a minimum eruption age is constrainable from the oldest sediments at Site 305, dated as Valanginian [29] (132–137 Ma [18]). Site 305 lies near magnetic anomalies M18 to M20 (143–146 Ma [18]), thus suggesting a lithospheric age of ~10 m.y. during eruption.

3. Plateau subsidence reconstructions

3.1. Paleo-water depths of sedimentation

To constrain plateau subsidence histories we must first estimate the depth of sedimentation at each drill site. Using a selection of sedimentary and microfossil data, especially benthic foraminifera, it is usually possible to discriminate between eight depth zones: subaerial, photic zone (depth = 0–50 m), shallow marine shelf above the storm wave base (0–200 m), upper bathyal below the storm wave base (200–500 m), mid bathyal (500–1500 m), lower bathyal (1500–3000 m), and abyssal (>3000 m). In addition, it is possible to assign depths in deep water relative to the lysocline and carbonate compensation depth (CCD) based on the preservation quality of calcareous microfossils.

We examine sediment descriptions in the ODP and DSDP site reports for the three plateaus: Ontong Java Plateau, Sites 288 and 289 [20], Sites 803 and 807 [30]; Manihiki Plateau, Site 317 [31]; and Shatsky Rise, Site 305 [29]. Stratigraphic age is determined using a combination of magnetostratigraphic and biostratigraphic data with the geologic time scales of Gradstein et al. [18] for the Cretaceous and Berggren et al. [32] for the Cenozoic. Fluctuations in eustatic sea level are ignored because the difference between present-day and pre-Aptian levels, which is most important to this study, is small (≤~150 m) [33] relative to the total subsidence and remains controversial [31]. For the deepest sedimentation zones of each drill site, we assume that the maximum deposition depths were no greater than the present-day seafloor depth. The shallowest and oldest paleo-water depth estimates at each site are the most important for constraining total plateau subsidence and are also the most reliable. Below, we describe our derivation of paleo-sedimentation depths for each drill site as illustrated graphically in Fig. 2.

3.1.1. Ontong Java Plateau site 288

Site 288 [20] sampled 988.5 m of primarily carbonate sediment, with the deepest portion of the core recovering lava cobbles and ash suggesting near-basement deposition. From the Coniacian to the present-day (0–89 Ma), slumped sediment facies and dissolution of foraminifera indicate deposition depths within the lysocline, but above the CCD. The Pacific CCD during the Campanian is estimated to have been at a depth of ~3700 m [34] and is expected to have been ~700 m shallower near topographic highs such as continents and oceanic plateaus [35]. By assuming the Cretaceous lysocline was 1000 m shallower than the CCD, as it is at present-day, we estimate the top of the Campanian lysocline to be ~2000 m. Thus for 0–89 Ma we estimate a minimum sedimentation depth at Site 288 of 2000 m and a maximum, equal to the present-day water depth of 3030 m. Turonian-Cenomanian (90–95 Ma) sediments show evidence for deposition between mid-bathyal depths and depths near the lysocline, which at these times is estimated to have been ~500 m deeper than in the Campanian [34]. We therefore estimate a depth range of 1000–2500 m for 90–95 Ma (Fig. 2). The oldest rocks recovered at Site 288 are Albian–Aptian (99–121 Ma) limestones with well preserved foraminifera and *Inoceramus* shells indicating water depths above the foraminifer lysocline, or shallower than ~1500 m. The shallowest possible deposition depth of the oldest sediments is estimated to be ~500 m based on the presence of clear pelagic facies, characteristic of depths below the upper bathyal zone.

3.1.2. Ontong Java Plateau site 289

Drilling at Site 289 [20] penetrated through the full 1262.5 m of sediment and 8.5 m into basaltic

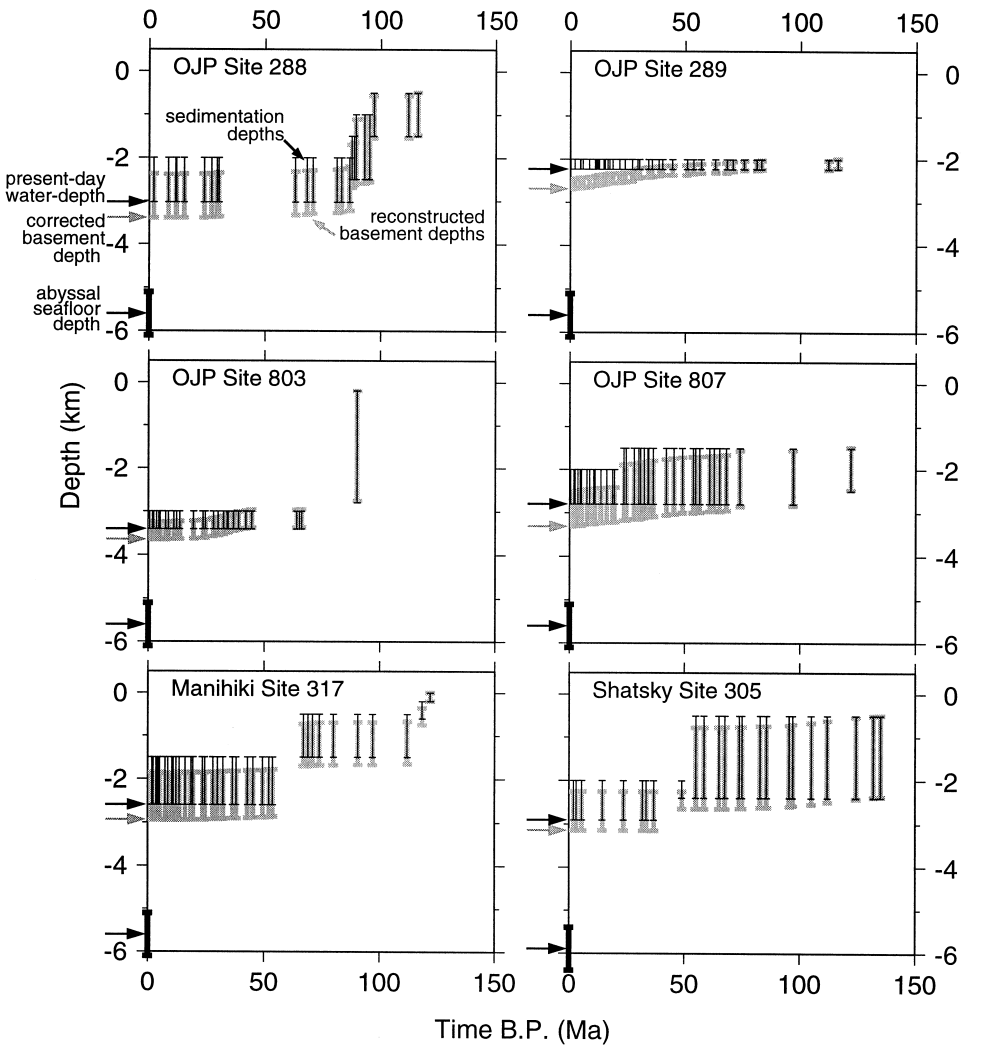

Fig. 2. Sediment-derived water depths as a function of sediment age at Sites 288, 289, 803, and 807 on the Ontong Java Plateau (OJP), Site 317 on the Manihiki Plateau and Site 305 on the Shatsky Rise. Vertical black bars show the range of possible values at each biostratigraphic date; gray bars are the depths of volcanic basement after removing the effects of sediment loading and compaction. The depth of the present-day plateau surface (upper black arrows) define the maximum bound depths for the deepest sedimentation zones. Gray arrows mark the sediment-unloaded basement depths, and lower black bars and arrows mark depths of sediment-unloaded basement of the surrounding abyssal seafloor.

basement. Throughout the entire sequence, sediment facies indicate very little change in water depth and suggest deposition near the CCD. Using the Pacific CCD reconstruction of Van Andel [34] and allowing for shallowing of the CCD near oceanic plateaus, we estimate sedimentation depths between 2000 m and the present-day depth of 2224 m (Fig. 2). This range is also consistent with near-basement micritic and chalky pelagic limestone, which indicates deposition below upper bathyal depths (i.e. >500 m), as well as non-vesicular pillow basalts, which require water depths >200 m [36].

3.1.3. Ontong Java Plateau site 803

At ODP Site 803 [30], volcanic basement was reached after 631 m of sediment penetration.

Eocene-to-recent sediments (0–54 Ma) show low proportions of benthic, relative to planktonic foraminifera, as well as abundant radiolarians, indicating water depths well within the lysocline. Late Cretaceous sediments overlying basement, however, are highly condensed and contain no calcareous microfossils, suggestive of water depths below the Cretaceous CCD, which we estimate to have been 3000 m near the plateau (∼700 m shallower than in the abyssal Pacific [35]). Since the Pacific CCD may have been significantly shallower in the Cenozoic than in the Cretaceous [34], it is unlikely that depths since the Eocene were greater than those in the Late Cretaceous. For times 0–66 Ma, we therefore estimate a minimum water depth of 3000 m and a maximum depth equal to the present-day depth of 3409 m. Unfortunately, a hiatus near the time of eruption (∼90 Ma) precludes sediment constraints on depths at this time; consequently, depth constraints are poor and rely on pillow basalts which show few or no vesicles and thus indicate depths ≥200 m.

3.1.4. Ontong Java Plateau site 807

Drilling at ODP Site 807 [30] sampled 1379 m of sediment before reaching volcanic basement. The upper part of the section contains pelagic limestones indicating deposition above the CCD. Sliter and Leckie [37] assigned a lower bathyal depth range on the basis of planktonic foraminifera, constraining the water depths to have been between 2000 m and the present-day value of 2805 m. Deposition appears to have been within the lysocline through the rest of the record, which limits depositional depths to 1500–2805 m. This depth range is reflected by the non-vesicularity of recovered pillow flows and is consistent with independent estimates based on CO_2 content of the sampled basalts (P. Michael, pers. commun. and [38]).

3.1.5. Manihiki Plateau site 317

On Manihiki, DSDP drilling reached basement at Site 317 [31]. The Cenozoic section here shows dissolution features on foraminifera [31] suggesting deposition near, or just within the lysocline. The lysocline was most likely deeper than 2000 m during this period, therefore a depth of 1500 m is allowed to be conservative. Deposition since 67 Ma is thus inferred to be below 1500 m and above the modern seafloor depth of 2598 m. Upper Cretaceous sediments comprise cherty carbonates with dissolution features, such as anomalously thin shelled bivalves. These observations indicate deposition in water depths greater than the storm-wave base (500 m) but at least intermittently near the lysocline (≤1500 m). Basement lavas show numerous, large vesicles, suggestive of eruption into unusually shallow water (<200 m [36]). In addition, Aptian volcaniclastic sediments overlying basement contain bivalves and gastropods of known shallow- to mid-shelf provenance (e.g., *Veniella* sp. [39]), although the lack of corals suggests depths below the photic zone (i.e. >50 m). These data indicate a relatively well constrained water depth range of 0–200 m shortly after volcanism.

3.1.6. Shatsky Rise, site 305

On the Shatsky Rise, DSDP Site 305 [29] penetrated through 640.5 m of sediment dating back to the Early Cretaceous. The sequence is dominated by cherty pelagic limestones. In the Neogene section of the core, the presence of radiolarians and partially dissolved calcareous fauna indicate deposition within the lysocline since 49 Ma [29]. Thus for times 0–49 Ma, we estimate deposition between 2000 m and the modern-day seafloor depth of 2903 m. Late Eocene-to-Cretaceous sediments show less dissolution but are still of predominantly pelagic facies, indicating deposition was deeper than the upper bathyal zone, but shallower than the Late Cretaceous lysocline. We therefore estimate a sedimentation depth range of 500–2400 m for 55–130 Ma.

3.2. Isostatic basement depth

In order to isolate the depth history of volcanic basement as driven only by mantle or accretionary processes we use the backstripping technique of Sclater and Christie [40], which subtracts the thickness of the sediments and removes their isostatic [12] load while taking into account the effects of sediment compaction. As illustrated in Fig. 2, sediment-unloaded basement depths are greater than depositional depths and increase with sediment column thickness or decreasing sediment age. This correction recovers an additional subsidence of 240–460 m

for Ontong Java, 340 m for Manihiki, and 240 m for Shatsky Rise.

The depth ranges shown in Fig. 2 mark the locus of possible isostatic basement depths during specific times at each drill site. The resolution of the reconstructed subsidence histories is limited by the uncertainties of the paleo-water depth estimates; the step-like subsidence patterns are the result of the discrete depth zones associated with characteristic sediment types and do not reflect the actual behavior of plateau subsidence.

3.3. Abyssal seafloor depths

Bathymetric swells of modern day hotspots affect broad regions (>1000 km [8]) of the seafloor extending well beyond the region of magmatism; therefore, an important constraint on the isostatic and thermal state of the lithosphere underlying oceanic plateaus is the depth of the adjacent abyssal seafloor. Near Ontong Java Plateau, we examine depths of the Nauru Basin to the east of the plateau which was drilled at DSDP Site 462 [41] and surveyed with reflection seismics [42]. After removing the loading effects of the ∼560 m of carbonate sediments and ∼470 m of Albian basalts, which post-date the original oceanic crust [43], we estimate a minimum sediment-unloaded basement depth of 5.7 km, compared to the uncorrected seafloor depth of 5.2 km. Given the significant topographic and stratigraphic variations documented in the Nauru Basin [42], we attribute an uncertainty of 0.5 km. For the abyssal seafloor adjacent to Site 317 on Manihiki Plateau, we estimate a sediment corrected depth of 5.63 km based on data from the nearest drill site, DSDP Site 595 [43], which was drilled in 5.60 km of water on the abyssal plain to the south of the Manihiki. Although the abyssal plain is relatively flat, stratigraphic data is limited; therefore, we estimate a 0.5 km uncertainty in this depth estimate. Near Shatsky Rise, the sediment-unloaded abyssal seafloor depth was assessed from DSDP Site 307 that drilled into the abyssal plain not far from the plateau [29]. The water depth at Site 307 is 5.7 km and the basement is covered by 300 m of pelagic sediment, which yields a corrected basement depth of 5.9 ± 0.5 km. We use the above isostatic depths as measures of the isostatic depth of the plume-affected lithosphere beneath each drill site.

3.4. Crustal topography

Crustal topography is the topography supported only by the thickened igneous crust. We define crustal topography at each drill site as the difference between the present-day sediment-unloaded basement depth and that of the adjacent abyssal seafloor. Crustal topography at Ontong Java ranges between 2 km, at Site 803 in the northeast, and 3 km, at Site 289 over the central portion of the plateau. Estimates of crustal topography on Manihiki at Site 317 and on Shatsky at Site 305 are both 2.7 km.

It is interesting to note that the above estimates of crustal topography are significantly less than estimates for modern-day hotspots such as Hawaii, in which Mauna Kea volcano stands 10 km above the surrounding seafloor (e.g. [44]); and Iceland, which stands ∼3.5 km above normal depths of the Mid-Atlantic Ridge [12]. The low topography of the Pacific plateaus may be surprising given that the documented crustal thicknesses are comparable or greater than thicknesses at Hawaii [45] and Iceland [46]. Flexural compensation by the rigid Pacific lithosphere at Hawaii [45], versus Airy isostatic compensation at Iceland and the oceanic plateaus [12] may account for much of the contrast with Hawaii. But Iceland is still significantly taller than the plateaus, especially when one considers the partially subaerial topography of Iceland which imposes a much greater load than the fully submarine relief of the plateaus. Neal et al. [13] attributes the low relief at Ontong Java to a thick layer of high-density lower crust, causing the plateau to sit deep in the mantle. This low relief may have been a factor in preventing the plateaus from reaching sea level [13,20,29–31] like their modern-day hotspot counterparts. Still, the cause of the low relief remains poorly understood. We do not focus on the cause of crustal topography here, rather we use the observed topography in conjunction with thermal models to predict changes in plateau depth since the crust was originally emplaced.

4. Thermal subsidence models

Subsidence of normal oceanic lithosphere is well explained by models in which initially hot and thin

lithosphere near a ridge axis cools and thickens approximately with the square root of age (e.g. [47, 48]). Subsidence of lithosphere affected by mantle plumes, however, departs significantly from that of normal lithosphere, as characterized by elevation of a hotspot swell, followed by subsidence to near normal depths over a period of several tens of millions of years once the lithosphere moves away from the plume source (e.g. [8,9]). A number of models have been developed to explain hotspot swell behavior and can be categorized as either isostatic or dynamic type models.

Isostatic models explain hotspot uplift by isostatic compensation of thermally expanded mantle and attribute the anomalous subsidence that follows to enhanced conductive cooling of the mantle (e.g. [8,9,49]). Crough [8] and Detrick and Crough [9] first proposed a lithospheric reheating model in which normal lithosphere is thinned by a plume such that it subsides like normal lithosphere of a younger age. Sleep [49] described a similar model, but also considered an anomalously hot layer of plume material injected at the base of the lithosphere. Dynamic swell models, on the other hand, explain hotspot uplift by viscous normal stresses imposed on the lithosphere by a rising mantle plume, and attribute the rapid subsidence to weakening stresses as the plume spreads and thins beneath the lithosphere (e.g. [5,10,50,51]). Both isostatic [9] and dynamic [10,50] type models have proven successful in explaining the ~1.5 km anomalous topography and subsidence of the Hawaiian swell.

In this study we use a simple isostatic, conductive cooling model. We consider one-dimensional thermal diffusion in which normal lithospheric cooling with age is interrupted by the injection of an anomalously hot mantle layer at the time t_0 that the hotspot is first active (Fig. 3a). The diffusion equation:

$$\frac{\partial T(t,z)}{\partial t} = \kappa \frac{\partial^2 T(t,z)}{\partial z^2} \quad (1)$$

where κ is thermal diffusivity, z is depth below the seafloor, t is seafloor age, and T is temperature, and is solved subject to the boundary conditions $T(t, z = 0) = 0$ºC and $T(t, z \geq L) = T_0$, where L is the final thickness of the lithospheric plate and T_0 is the reference mantle temperature. In the absence of a hotspot, the initial condition of $T(t = 0, z > 0) = T_0$ eventually cools to a conductive temperature gradient in the lithospheric plate. This causes normal seafloor subsidence. We consider respective values of κ (8.1×10^{-7} m^2/s), T_0 (1350ºC, 1450ºC), coefficient of thermal expansion (3.28×10^{-5}, 3.1×10^{-5}), plate thickness L (125 km, 95 km), and zero-age depth (2.5 km, 2.6 km) of the end-member plate cooling models of Parsons and Sclater [48] and Stein and Stein [47].

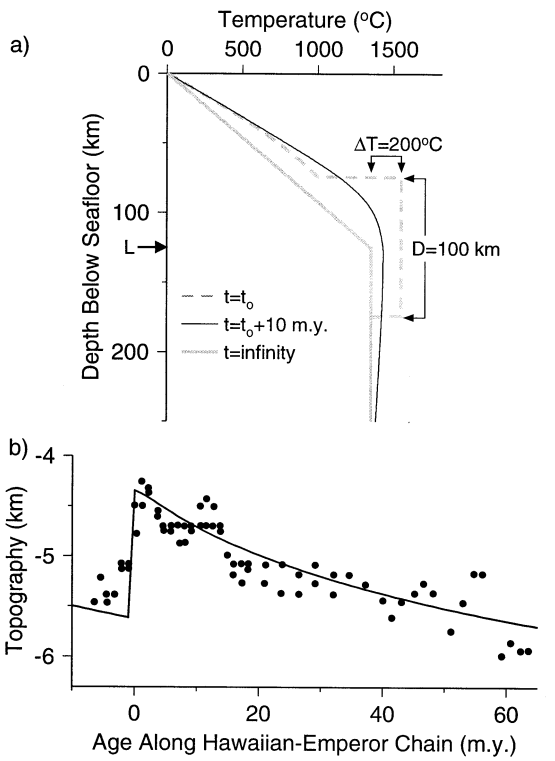

Fig. 3. (a) Mantle geotherms predicted in simulations of hotspot-affected mantle. This example is our model of the Hawaiian swell in which normal conductive cooling is interrupted by the injection of an anomalously hot mantle layer with average temperature anomaly $\Delta T = 200$ºC and thickness $D = 100$ km (dashed curve). After 10 m.y., heat diffusion reduces temperature anomalies (black curve) which causes swell subsidence. Finally, at infinite age, the mantle cools to a conductive geotherm above a constant temperature asthenosphere (gray curve). (b) Predictions of the thermal model described in (a) are consistent with the observed depth–age relationship of the Hawaiian hotspot and seamount chain (dots) [9].

To predict anomalous thermal uplift and subsidence of hotspot-affected lithosphere, we begin with the same initial conditions as above for normal litho-

sphere, but at a specified age t_0, we introduce a mantle layer with an anomalous temperature ΔT and a thickness D beneath the 1000ºC isotherm (Fig. 3a). From time t_0, we allow temperatures to decay to the conductive geotherm of the normal lithospheric plate (Fig. 3a). This model thus simulates the instantaneous delamination and plume replacement of mantle hotter than 1000ºC [52], and subsequent heat dissipation.

The most important prediction of our thermal subsidence models for comparison with the reconstructed subsidence values is the initial hotspot uplift (i.e. uplift at $t = t_0$), which is controlled primarily by the parameters ΔT and D. The large igneous volumes of the Ontong Java, Manihiki, and Shatsky Plateaus (1–4 $\times$ 10^7 km^3 [1,25]) suggest a hotspot source with effective ΔT and D at least as significant as those of modern-day hotspots such as Hawaii (igneous volume $\sim$ 5 $\times$ 10^6 km^3 assuming isostatic equilibrium of eight major islands [44]) and Iceland (igneous volume $\sim$ 1 $\times$ 10^7 km^3 [25]). Estimates of ΔT and D for modern-day plumes range from $\Delta T \sim 200$ºC and $D \sim 100$ km as typical of isostatic models (e.g. [49], to $\Delta T \sim 300$ºC for dynamic models [10,50].

As a reference model, we first simulate the amplitude and subsidence of the Hawaiian swell. To account for the rapid subsidence following initial uplift (Fig. 3b), we increase thermal diffusivity in the asthenosphere by a factor of 15 which, in an ad hoc fashion, compensates for the advective heat loss that would occur due to vertical thinning of plume material ponding beneath the lithosphere. Our enhancement factor simulates a Peclet number ($Pe = WD/\kappa$) of 15, where W is the average thinning rate of the plume. Although this thinning rate may be very high for low-viscosity plumes (Sleep's [51] thinning rate of $\sim$10 km/m.y. implies a Pe of $\sim$30 for $D = 100$), we choose Pe such that our models predict subsidence rates consistent with that observed of the Hawaiian plume. As shown in Fig. 3b, this reference model reproduces successfully the Hawaiian swell initial uplift of $\sim$1.5 km and later subsidence with the parameters $\Delta T = 200$ºC and $D = 100$ km.

For application to the plateau hotspots, we assume lower-bound parameters of $\Delta T = 150$ºC and $D = 100$ km, and upper-bound values of $\Delta T = 350$ºC [5] and $D = 200$ km. The low plume temperature anomalies and thicknesses yield initial swell uplifts of $\sim$1.0 km as consistent with the lower-bound estimates of Griffiths et al. [11]; while the high plume temperature anomalies and thicknesses predict uplifts of 2-3 km, still conservative relative to the 3-4 km uplifts predicted by Farnetani and Richards' [5] dynamic plume-head models. Lithospheric age at the time of plume initiation t_0 is the age contrast between the adjacent seafloor (extrapolated from isochrons to each drill site) and the oldest basalt sampled on each plateau.

5. Comparison of predicted thermal and reconstructed subsidence values

As illustrated in Fig. 4, the observed abyssal seafloor depths indicate little or no bathymetric anomaly relative Parsons and Sclater's [48] predictions of normal seafloor (Stein and Stein's [47] model predicts an even closer match). The hotspot curves are consistent with this result; they predict the anomalous hotspot topography to have diminished to negligible values at present-day. To examine the depth histories of the plateaus, we correct for the crustal topography by shifting the hotspot subsidence curves to the present-day sediment-unloaded basement depths at each drill site. We also take into account the excess load of subaerial, versus submarine topography when the plateau is predicted to be above sea level (Fig. 4). In this crustal topography correction we are assuming that all the crust that exists at present-day erupted rapidly at the time of plume initiation.

We find that when both reconstructed and predicted plateau depths exceed $\sim$1 km, such as during the last $\sim$100 m.y. of the drill sites and the whole sedimentary history of Site 803, the model depths are consistent with the large ranges allowable by the reconstructions (Fig. 4). At the greatest ages, however, when hotspot topography is predicted to be highest, resolvable differences between reconstructions and model predictions become apparent. At Site 288, the predicted depths of only the mild-temperature plume anomalies are consistent with the shallowest reconstructed depths, while the high-temperature plume models predict subaerial eruptions that are clearly precluded by the marine sediments indicating depths

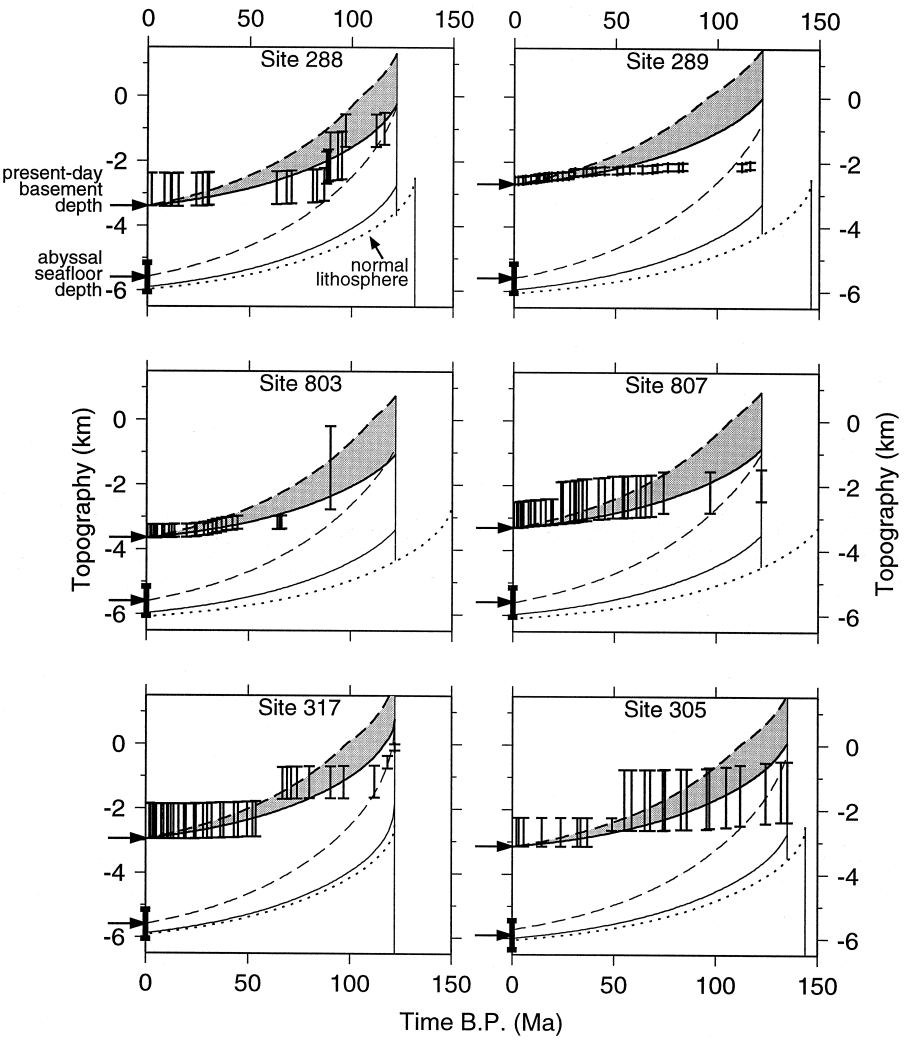

Fig. 4. Thermal subsidence predictions using model parameters of Parsons and Sclater [48] are compared with reconstructed basement depths (vertical bars) at each drill site. Subsidence predicted from mild-temperature plumes (solid curves, $\Delta T = 150$ºC, $D = 100$ km) and high-temperature plumes (dashed curves, $\Delta T = 350$ºC, $D = 200$ km) are shown for the abyssal seafloor (lower) and plateau surface (upper and shaded) (see text for further description). The shaded area represents depths due to plumes intermediate between our mild- and high-temperature plume end-members. The dotted curve marks the subsidence of normal lithosphere [48]. Also marked are present-day depths of sediment-unloaded basement of the plateaus (upper arrows), which define the maximum bound depth of the reconstructions, and adjacent abyssal seafloor (black bars and arrows).

below the photic zone. At Site 289, 807, 317, and 305 even the mild-temperature plume models predict topography to exceed the shallowest reconstructed estimates. In fact, the mild-temperature plume models of Sites 289, 317, and 305 predict eruptions to have been subaerial whereas the drill sites showed only marine sedimentation — even in deep water, as in the case of 289 and 305.

The differences between reconstructions and predictions become more clear when we examine total subsidence (Fig. 5). Total subsidence is the most robust quantity of both model predictions and paleo-depth reconstructions. In model predictions, the end-member parameters of Parsons and Sclater [48] and Stein and Stein [47] yield upper- and lower-bound subsidence predictions, respectively. In re-

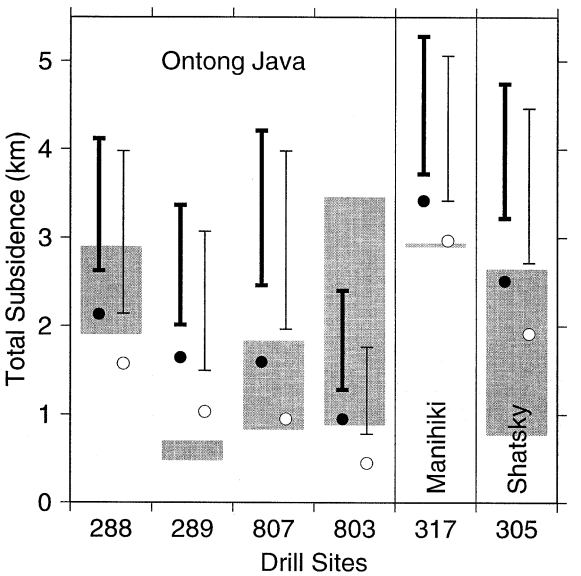

Fig. 5. Total subsidence estimates from sediment reconstructions (gray boxes denote range of upper to lower bounds) are compared with predictions of thermal models of hotspot-affected (bar lengths mark ranges predicted of mild- to high-temperature plumes) and normal seafloor (circles). The two sets of symbols show results using plate cooling parameters of Parsons and Sclater [48] (bold bars and solid circles) and of Stein and Stein [47] (thin bars and open circles).

constructions, the uncertainty in depth of the oldest sediments determine the uncertainty in total reconstructed subsidence. At Site 803 the model predictions are consistent with the poor constraints from the drill core data, whereas at Site 288, only the mild-temperature plume predictions are consistent with the reconstructions. The other drill sites appear to have subsided resolvably less than predicted from the mild-temperature plume models and significantly less than predicted from the hot plume models. In fact, the reconstructed subsidence values appear to be most consistent with the values predicted by normal lithosphere, a conclusion noted by Neal et al. [13] for Ontong Java and noted by Coffin [53] for the Indian Ocean Plateaus. Thus, the largest of the worlds oceanic plateaus show little or no evidence for the anomalous uplift and subsidence that is predicted by thermal models which assume rapid crustal emplacement.

6. Uncertainties and implications for moderate plume anomalies

A number of factors may contribute to the ~1-km discrepancy in total subsidence between drill core reconstructions and lower-bound model predictions. One possibility is that actual basement depths were shallower and thus total subsidence was greater than estimated from the drill core reconstructions. Indeed, the depths of the oldest sediments, which is most important to total subsidence estimates, vary in degree of uncertainty. At Manihiki, for example, the depths of the oldest sediments are particularly well constrained by the very shallow water sediments at Site 317; therefore, it is unlikely that Site 317 subsided significantly more than we have estimated. At Sites 288 and 305, depths of the oldest sediments are less well constrained by intermediate-depth sediments; however, it is unlikely that sedimentation occurred more than a few hundred meters shallower than we have estimated given the lack of shallow water sediments. At Sites 289 and 807, depth estimates are limited by uncertainties in the depth of the lysocline. Another factor that may have contributed to errors in paleodepth estimates is variations in eustatic sea level. If indeed, sea level in pre-Aptian times was as much as 150 m shallower than today [33], then we may be under-estimating total subsidence by a comparable amount. Together, the uncertainties in sedimentation depth and sea level could allow for an additional ~0.5 km of subsidence thus bringing reconstructed values closer to the predictions of the plume models.

Another possibility is that our thermal models are over-predicting the actual subsidence of the plateaus. One source of uncertainty is the relative ages between the plateau and surrounding seafloor. For example, if the plateaus erupted on seafloor 10 m.y. older than we have modeled, then this would reduce subsidence predictions for mild-temperature plumes by as much as 0.2–0.3 km for Ontong Java, 0.8 km for Manihiki, and 0.6 km for Shatsky, all else being equal. On the other hand, eruption on younger seafloor would substantially increase subsidence predictions. Another factor that could reduce predicted subsidence values is the possibility that the eruptions at the drill sites did not coincide, both in time and in geographic location, with the maximum in swell uplift. Dynamic models of Farnetani and Richards

[5], for example, predict the completion of magmatic activity to post-date the peak in lithospheric uplift by ~10 m.y., in which time swell topography diminishes by 10–30%. Such models also predict swell topography to decrease with radial distance away from the center of the swell. Thus, the subsidence at the individual drill sites might reflect a smaller local subsidence than the maximum hotspot subsidence that we consider in our model predictions. This possibility, however, may be difficult to reconcile at Sites 289, 317, and 305, which show little subsidence despite being centrally located within the plateaus.

Yet another factor that may account for the low apparent subsidence is recent uplift due to processes unrelated to the original hotspot source. Ontong Java may have been uplifted by the passage over the Samoa hotspot at ~40–50 Ma [17]. However, at present-day, this additional uplift is likely to be small if the Samoa swell subsided at rates comparable to the Hawaii swell. A more likely source of presently-active uplift at Ontong Java is the flexural bending of the Pacific Plate due to subduction beneath the Solomon Trench [54]. Still, this possibility is difficult to reconcile with the fact that the drill site closest to the trench (Site 288, Fig. 1) appears to have experienced the greatest amount of subsidence since accretion.

Thus, the above uncertainties in depth reconstructions, model predictions, and additional geologic effects could account for a ~1 km discrepancy between reconstructed subsidence estimates and the values predicted by models of rapid crustal emplacement over mild-temperature plumes (Fig. 5). On one hand, a ~1 km swell height implies that the plumes which gave rise to these large igneous provinces may have been comparable in volume and temperature to those of modern day plumes such as at Hawaii and Iceland. On the other hand, the extreme volume of magmatism and the inferred high extents of melting [16] suggests a plume source of greater volume and higher temperature. Yet we find little evidence for the uplift of 2–3 km that is predicted from rapid crustal emplacement of high temperature plumes or plume heads. Subsidence of ~4 km, as predicted by large-radius (400 km [1]) dynamic plume-head models [5], is even more unlikely. We are thus left with the task of explaining how a high temperature and volume plume can yield only low subsidence.

7. Prolonged igneous underplating

In our thermal model predictions above, we have assumed that all of the present-day crustal topography was emplaced rapidly near the peak in hotspot uplift. The prediction of Farnetani and Richards' [5] dynamic models that plateau magmatism continues well beyond the peak in dynamic uplift offers an alternative hypothesis that may account for the low subsidence: The depth histories of the plateaus reflect, in addition to mantle subsidence, uplift due to prolonged or later-stage crustal growth in the form of intrusions, underplating the plateaus. This uplift due to underplated magmas would reduce the subsidence of the plateau surfaces relative to that caused by mantle cooling and therefore could allow for a high temperature and volume plume source to yield low subsidence values. Furthermore, the possibility that accretion was incomplete at the time of plume initiation may have been an additional factor that prevented the plateaus from reaching sea level.

Hard evidence for at least one major late-stage extrusive event on Ontong Java is the $^{40}Ar/^{39}Ar$ dates of 90 Ma obtained at Site 803 and the Solomon Islands [17]; even later-stage events are evident by the dates of ~63 and ~34 Ma found on the Solomon Islands [17]. On Manihiki, evidence for later-stage magmatism is the 69.5 Ma date obtain on Mt. Eddie seamount [55]. Volcanic basement of Shatsky Rise still remains to be dated. Possible evidence for underplating is the high-seismic velocities observed in the lower crust of Ontong Java (e.g. [1,13–15]) as well as beneath Manihiki and Shatsky [14]. However, Neal et al. [13] also argues that a significant volume of this high velocity lower crust is the remnant crystallization product of the extruded magmas. Nonetheless, magmatic underplating is thought to be an important component in the construction of hotspot islands and other flood basalt provinces (e.g. [1]) and likewise, might be important to the construction of oceanic plateaus.

Another strength of the late-stage underplating hypothesis is that it may explain many of the normal faults observed throughout Ontong Java [14,20], Manihiki [22], and Shatsky (W. Sager, pers. commun.). Because underplating is predicted to isostatically uplift the plateau surface relative to the surrounding seafloor, this may have produced

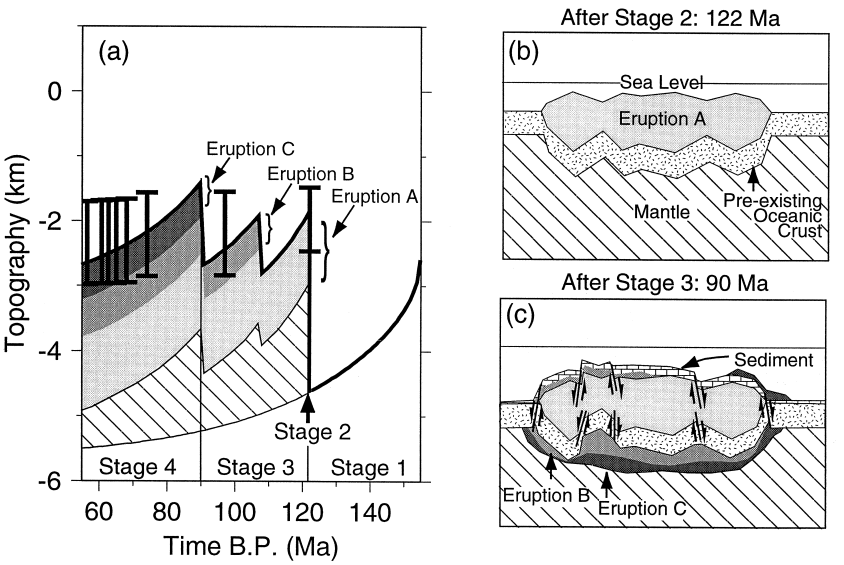

Fig. 6. (a) This diagram illustrates a hypothetical multi-staged accretion scenario as compared with reconstructed depths at Ontong Java Site 807. The bold curve marks the evolution of the plateau's volcanic surface and the hachured region denotes the predicted anomalous uplift of the surrounding seafloor (i.e. just mantle topography) above a normal subsidence curve. Crustal topography of the first magmatic event (eruption A) is denoted by light shading, the second magmatic event (eruption B) is denoted by medium shading, and the third magmatic event (eruption C) is denoted by dark shading. (b) This cartoon illustrates schematic crustal structure after the initial magmatic event. Crust emplaced by eruption A is the light shading, pre-existing oceanic crust is dotted, and mantle is hachured. (c) Structure at the completion of plateau construction. Underplated and extruded crust emplaced during eruption B is the medium shading and crust emplaced during the final eruption C is the dark shading. Late stage underplating magmas cause plateau uplift relative to the seafloor which is accommodated by extensive normal faulting (arrows).

widespread, late stage faulting. Indeed, many faults on Manihiki are known to cut through appreciable sections of the sediments thus indicating faulting occurred well after basement emplacement [22]. Furthermore, this source of faulting does not require fault orientations to coincide with tectonic fabric, therefore, does not require complex ridge geometries which may otherwise be necessary to explain the fault patterns observed on the Ontong Java [19] and Manihiki [22] Plateaus.

If the difference between predicted and reconstructed subsidence is attributed all to later-stage underplating, then a significant volume of the existing crust at these plateaus might be underplated material. Underplating relative to extrusive crust may be as much as 50% for Ontong Java, 30% for Manihiki, and 20% for Shatsky as implied by differences between the maximum reconstructed and the minimum (mild-plume) predicted subsidence values. Predictions of the high-temperature plumes would suggest even higher percentages of underplating.

Fig. 6 illustrates schematically our hypothesized accretion scenario incorporating late-stage magmatic underplating and its consequences on surface morphology. We use the reconstructed depths of Ontong Java Site 807 in our hypothetical example (Fig. 6a). Stage 1 is before plateau accretion, when the seafloor subsides due to normal lithospheric cooling. Stage 2 is the impact of the mantle plume or plume head beneath the lithosphere, causing thermal uplift and the initial pulse of magmatic accretion (Eruption A; Fig. 6a and b). During Stage 3, a time-dependent mantle source may have caused episodic uplift accompanied by underplating, and in a few places, surface extrusion (Fig. 6a) as documented by the later-stage events recorded at Ontong Java (90 Ma) and Manihiki (~70 Ma). Underplated magma, with density less than that of mantle, causes uplift relative to the surrounding abyssal seafloor, so that the plateau subsides to a lesser degree than the surrounding lithosphere and is broken by extensive normal faults (Fig. 6a and c). Finally, in Stage 4, the hotspot

either becomes inactive or the plateau is removed from its vicinity by plate motion, so that both plateau and surrounding seafloor subside together as the underlying mantle cools. A continuous rather than a step-wise underplating scenario would also be consistent with the existing subsidence data.

8. Discussion

The prolonged accretionary scenario proposed above may have implications for the dynamics and magmatic productivity of the Cretaceous mantle. Previous theoretical studies have examined the possible geodynamic causes of a multiple-staged growth history. For example, Bercovici and Mahoney [56] demonstrated that a buoyant plume ascending from the core–mantle boundary will tend to break into two separate plume heads which impact the surface at different times. Another model by Larson and Kincaid [57], explains a two-pulsed magmatic accretion by a convection instability of the 670 km discontinuity, followed by the ascent of a plume from the lower mantle, both of which are caused by increased flux of subduction slabs into the lower mantle.

The difficulty with such prolonged accretion scenarios, as well as with our underplating model, is that they imply very little motion between the plate and mantle source over the duration of accretion. A slow moving plate at Ontong Java between 122 and 90 Ma is consistent with plate reconstructions, showing Ontong Java very near the Pacific Plate's pole of rotation during most of this time period [13]. On the other hand, this rotation pole would require Manihiki and Shatsky to have moved substantially during these times. Constraints on Pacific Plate motion before 100 Ma, however, are based largely on paleo-magnetic studies (e.g. [28]) which have large uncertainties compared to constraints based on geographic age progressions of dated basalt samples.

Another implication of a prolonged growth history is the suggestion that initial magmatic fluxes may have been smaller than estimated previously [1–3]. A multiple-staged growth history implies two or more major magmatic pulses whereas the previous estimates assumed all the crust was emplaced in a single ~3 m.y. pulse. A continuous growth history suggests that magmatism occurred continuously over 10–30 m.y. Such a scenario could reduce magmatic flux estimates by an order of magnitude and thus implies environmental impacts significantly less than previously hypothesized [58].

Given the uncertainties associated with our analyses as well as the sparse sampling of these giant oceanic edifices, it is clear that further studies are needed. More extensive sampling would help constrain magmatic budgets and possibly identify new phases of surface eruption, necessary to test models of stepped versus continuous accretion. In addition, further bathymetric, gravity, and crustal seismic observations will provide better constraints on crustal volume and density partitioning, as well as reveal the structure and mechanisms of faulting.

9. Conclusions

The sedimentary sequences at six DSDP/ODP sites record depths of the Ontong Java, Manihiki, and Shatsky Plateaus from the time of accretion to present-day. The drilled sediments indicate that the plateaus may have subsided only as much as normal seafloor and significantly less than predicted by models of hotspot-affected lithosphere. If crustal emplacement was rapid, uncertainties allow for the ~1 km of anomalous subsidence expected from a mantle source comparable in temperature and size to the sources of modern-day hotspots such as Hawaii and Iceland. However, it is difficult, with a rapid emplacement scenario, to account for the 2–3 km of anomalous subsidence predicted for high-temperature, high-volume sources which may be required to explain the large volumes of these giant igneous edifices.

An alternative possibility is that the subsidence histories reflect the superposition of (1) anomalous mantle subsidence from the plume source, and (2) additional uplift due to prolonged, later-phase underplating. This prolonged underplating scenario is consistent with the findings of later-phase surface eruptions on the Ontong Java and Manihiki Plateaus; it may account for much of the high seismic-velocity crust observed beneath the three plateaus; and it may explain the widespread normal faults throughout and along their margins. Prolonged crustal growth also predicts the original crustal topography at the time of

plume initiation to be even less than it is at present day, and thus provides an explanation for why these plateaus failed to reach sea level. Finally, a prolonged accretionary scenario for these oceanic flood basalt provinces implies little relative motion between the mantle source and lithospheric plates during the period of accretion, and suggests that eruptions rates may have been less than previously believed.

Acknowledgements

This study was supported by funds from the Woods Hole Oceanographic Institution and the University of Hawaii, SOEST Young Investigator Program. We extend our thanks to our editor C. Langmuir as well as to J. Caplan-Auerbach, R. Larson, J. Mahoney, S. Stein, and three anonymous reviewers for their insightful comments to this manuscript. Contribution numbers WHOI-9708 and SOEST-4633. *[CL]*

References

[1] M.F. Coffin, O. Eldholm, Scratching the surface: Estimating dimensions of large igneous provinces, Geology 21 (1993) 515–518.
[2] J.A. Tarduno, W.V. Sliter, L.W. Kroenke et al., Rapid formation of Ontong Java Plateau by Aptian mantle plume volcanism, Science 254 (1991) 399–403.
[3] M.A. Richards, R.A. Duncan, V.E. Courtillot, Flood basalts and hotspot tracks: Plume heads and tails, Science 246 (1989) 103–107.
[4] I.H. Campbell, R.W. Griffiths, Implications of mantle plume structure for the evolution of flood basalts, Earth Planet. Sci. Lett. 99 (1990) 79–93.
[5] C.G. Farnetani, M.A. Richards, Numerical investigations of the mantle plume initiation model for flood basalt events, J. Geophys. Res. 99 (1994) 13813–13833.
[6] J.J. Mahoney, An isotopic survey of Pacific oceanic plateaus: Implications for their nature and origin, in: B. Keating, P. Fryer, R. Batiza, G.W. Boehlert (Eds.), Seamounts, Islands, and Atolls, Am. Geophys. Union Monogr. Ser. Vol. 43, Washington, D.C., 1987, pp. 207–220.
[7] J.J. Mahoney, K.J. Spencer, Isotopic evidence for the origin of the Manihiki and Ontong Java ocean plateaus, Earth Planet. Sci. Lett. 104 (1991) 196–210.
[8] S.T. Crough, Thermal origin of mid-plate hot-spot swells, Geophys. J. R. Astron. Soc. 55 (1978) 451–469.
[9] R.S. Detrick, S.T. Crough, Island subsidence, hot spots, and lithospheric thinning, J. Geophys. Res. 83 (1978) 1236–1244.
[10] P. Olson, Hot spots, swells and mantle plumes, in: M.P. Ryan (Ed.), Magma Transport and Storage, Wiley, Chichester, 1990, pp. 33–51.
[11] R.W. Griffiths, I.H. Campbell, Interaction of mantle plume heads with the Earth's surface and onset of small-scale convection, J. Geophys. Res. 96 (1991) 18295–18310.
[12] D.T. Sandwell, K.R. MacKenzie, Geoid height versus topography for oceanic plateaus and swells, J. Geophys. Res. 94 (1989) 7403–7418.
[13] C.R. Neal, J.J. Mahoney, L.W. Kroenke, R.A. Duncan, M.G. Petterson, The Ontong Java Plateau, in: J.J. Mahoney, M.F. Coffin (Eds.), Large Igneous Provinces, Am. Geophys. Union Monogr., Washington, D.C., 1997, pp. 183–216.
[14] D.M. Hussong, L.K. Wipperman, L.W. Kroenke, The crustal structure of the Ontong Java and Manihiki oceanic plateaus, J. Geophys. Res. 84 (1979) 6003–6010.
[15] T.P. Gladczenko, M.F. Coffin, O. Eldholm, Crustal structure of the Ontong Java Plateau: Modeling of new gravity and existing seismic data, J. Geophys. Res. 102 (1997) 22711–22729.
[16] J.J. Mahoney, M. Storey, R.A. Duncan, K.J. Spencer, M. Pringle, Geochemistry and age of the Ontong Java Plateau, in: M. Pringle, W. Sager, W. Sliter, S. Stein (Eds.), The Mesozoic Pacific, Geophys. Monogr. Ser. Vol. 77, Washington, D.C., 1993, pp. 233–261.
[17] M.L.G. Tejada, J.J. Mahoney, R.A. Duncan, M.P. Hawkins, Age and geochemistry of basement and alkalic rocks of Malaita and Santa Isabel, Solomon Islands, southern margin of Ontong Java Plateau, J. Petrol. 37 (1996) 361–394.
[18] F.M. Gradstein, F.T. Agterberg, J.G. Ogg et al., A Triassic, Jurassic and Cretaceous time scale, in: W.A. Berggren, D.V. Kent, M.P. Aubry, J. Hardenbol (Eds.), Geochronology, Timescales and Global Stratigraphic Correlation, Soc. Econ. Paleontol. Mineral., 1995, pp. 95–126.
[19] E.L. Winterer, M. Nakanishi, Evidence for a plume-augmented, abandoned spreading center on Ontong Java Plateau, Eos Trans. AGU, 76 (46) (1995) 617, Fall Meet. Suppl.
[20] J.E. Andrews, G.H. Packham, Initial Reports Deep Sea Drilling Project, 30, Washington, D.C., 1975.
[21] W.H.F. Smith, D.T. Sandwell, Marine gravity field from declassified Geosat and ERS-1 altimetry, Eos Trans. AGU, 76 (1995) 156, Fall Meeting Suppl.
[22] E.L. Winterer, P.F. Lonsdale, J.L. Mathews, B.R. Rosendahl, Structure and acoustic stratigraphy of the Manihiki Plateau, Deep-Sea Res. 21 (1974) 793–814.
[23] M.A. Lanphere, G.B. Dalrymple, K–Ar ages of the basalts from DSDP Leg 33: Site 315 (Line Islands) and 317 (Manihiki Plateau), Initial Reports Deep Sea Drilling Project, 33, Washington, D.C., 1976.
[24] M. Caron, Cretaceous planktonic foraminifera, in: H.M. Bolli, J.B. Saunders, K. Perch-Nielsen (Eds.), Plankton Stratigraphy, Cambridge University Press, Cambridge, 1985, pp. 17–86.
[25] G. Schubert, D. Sandwell, Crustal volumes of the conti-

nents and of oceanic and continental submarine plateaus, Earth Planet. Sci. Lett. 92 (1989) 234–246.
[26] M. Nakanishi, E.L. Winterer, Tectonic events of the Pacific Plate related to formation of Ontong Java Plateau, Eos Trans. AGU, 77 (1996) 705-706, Fall Meeting Suppl.
[27] M. Nakanishi, K. Tamaki, K. Kobayashi, Mesozoic magnetic anomaly lineations and seafloor spreading history of the northwestern Pacific, J. Geophys. Res. 94 (1989) 15437–15462.
[28] W.W. Sager, H.-C. Han, Rapid formation of the Shatsky Rise oceanic plateau inferred from its magnetic anomaly, Nature 364 (1993) 610–613.
[29] R.L. Larson, R. Moberly and Shipboard Scientific Party, Initial Reports Deep Sea Drilling Project, 32, Washington, D.C., 1975.
[30] L.W. Kroenke, W.H. Berger, T.R. Janecek and Shipboard Scientific Party, Proc. Ocean Drilling Program, Initial Reports, 130, College Station, TX, 1991.
[31] S.O. Schlanger, E.D. Jackson, Initial Reports Deep Sea Drilling Project, 33, Washington, D.C., 1976.
[32] W.A. Berggren, D.V. Kent, C.C. Swisher, M.P. Aubry, A revised Cenozoic Geochronology and Chronostratigraphy, in: W.A. Berggren, D.V. Kent, M.P. Aubry, J. Hardenbol (Eds.), Geochronology, Timescales and Global Stratigraphic Correlation, Soc. Econ. Paleontol. Mineral., Spec. Publ., 1995, pp. 129–212.
[33] B.U. Haq, J. Hardenbol, P.R. Vail, Chronology of fluctuating sea levels since the Triassic, Science 235 (1987) 1156–1167.
[34] T.H.V. Andel, Mesozoic/Cenozoic compensation depth and the global distribution of calcareous sediments, Earth Planet. Sci. Lett. 26 (1975) 187–194.
[35] W.H. Berger, E.L. Winterer, Plate stratigraphy and the fluctuating carbonate line, in: K.J. Jsu, H.C. Jenkyns (Eds.), Pelagic Sediments: On Land and Under the Sea, Int. Assoc. Sedimentol., Spec. Publ., 1974, pp. 11–48.
[36] J.G. Moore, J.G. Schilling, Vesicles, water, and sulfur in Reykjanes Ridge basalts, Contrib. Mineral. Petrol. 41 (1973) 105–118.
[37] W.V. Sliter, R.M. Leckie, Cretaceous planktonic foraminifera and depositional environments from the Ontong Java Plateau, Ocean Drilling Program, Initial Reports, 130, College Station, TX, 1993.
[38] P.J. Michael, W.C. Cornell, H_2O, CO_2, Cl and S contents in 122 Ma glasses from Ontong Java Plateau, ODP 807C: Implications for mantle and crustal processes, Trans. Am. Geophys. Union, 77 (1996) 714, Fall Meeting Suppl.
[39] E.G. Kauffman, Deep sea Cretaceous macrofossils: Hole 317A, Manihiki Plateau, Initial Reports Deep Sea Drilling Project, 33, Washington, D.C., 1976.
[40] J.G. Sclater, P.A.F. Christie, Continental stretching: an explanation of the post Mid-Cretaceous subsidence of the central North Sea basin, J. Geophys. Res. 85 (1980) 3711–3739.
[41] R.L. Larson, S.O. Schangler and Shipboard Scientific Party, Initial Reports Deep Sea Drilling Project, 61, Washington, D.C., 1981.
[42] T.H. Shipley, L.J. Abrams, Y. Lancelot, R.L. Larson, Late Jurassic–Early Cretaceous oceanic crust and early Cretaceous volcanic sequences of the Nauru Basin, in: M. Pringle, W. Sager, W. Sliter, S. Stein (Eds.), The Mesozoic Pacific, Geophys. Monogr. Ser. Vol. 77, Washington D.C., 1993, pp. 233–261.
[43] H.W. Menard, J.H. Natland and Shipboard Scientific Party, Initial Reports Deep Sea Drilling Project, 91, Washington, D.C., 1987.
[44] D.A. Clague, G.B. Dalrymple, The Hawaiian–Emperor Volcanic Chain, in: R.W. Decker, T.L. Wright, P.H. Stauffer (Eds.), Volcanism in Hawaii, USGS Prof. Pap., 1350 (1987) 5–54.
[45] A.B. Watts, U.S. ten Brink, P. Buhl, T.M. Brocher, A multichannel seismic study of lithospheric flexure across the Hawaiian–Emperor seamount chain, Nature 315 (1985) 105–111.
[46] R.K. Staples, R.S. White, B. Branksdóttir et al., Färoe–Iceland ridge experiment 1. Crustal structure of northeastern Iceland, J. Geophys. Res. 102 (1997) 7849–7866.
[47] C.A. Stein, S. Stein, A model for the global variation in oceanic depth and heat flow with lithospheric age, Nature 359 (1992) 123–129.
[48] B. Parsons, J.G. Sclater, An analysis of the variation of ocean floor bathymetry and heat flow with age, J. Geophys. Res. 82 (1977) 803–827.
[49] N.H. Sleep, Hotspots and mantle plumes: Some phenomenology, J. Geophys. Res. 95 (1990) 6715–6736.
[50] N.M. Ribe, U.R. Christensen, Three-dimensional modelling of plume–lithosphere interaction, J. Geophys. Res. 99 (1994) 669–682.
[51] N.H. Sleep, Lateral flow and ponding of starting plume material, J. Geophys. Res. 102 (1997) 10001–10012.
[52] N.H. Sleep, Lithospheric thinning by midplate mantle plumes and the thermal history of hot plume material ponded at sublithospheric depths, J. Geophys. Res. 99 (1994) 9327–9343.
[53] M.F. Coffin, Emplacement and subsidence of Indian Ocean plateaus and submarine ridges, in: R.A. Duncan, D.K. Rea, R.B. Kidd, U. von Rad, J.K. Weissel (Eds.), Synthesis of Results from Scientific Drilling in the Indian Ocean, Am. Geophys. Union Geophys. Monogr. Ser. Vol. 70, 1992, pp. 115–125.
[54] P. Coleman, L. Kroenke, Subduction without volcanism in the Solomon Islands arc, Geo-Mar. Lett. 1 (1981) 129–134.
[55] H. Beiersdorf, J. Erzinger, Observations on the bathymetry and geology of the northeastern Manihiki Plateau, southwestern Pacific Ocean, South Pac. Mar. Geol. Notes, CCPO/SOPAC, 1989, pp. 33–46
[56] D. Bercovici, J. Mahoney, Double flood basalts and plume head separation at the 660-kilometer discontinuity, Science 266 (1994) 1367–1369.
[57] R.L. Larson, C. Kincaid, Onset of mid-Cretaceous volcanism by elevation of the 670 km thermal boundary layer, Geology 24 (1996) 551–554.
[58] R.L. Larson, Geological consequences of superplumes, Geology 19 (1991) 963–966.